68 $LiNH_4C_4H_4O_6 \cdot H_2O$ family

68A Pure compounds

No. 68A-1 $LiNH_4C_4H_4O_6 \cdot H_2O$, Lithium ammonium tartrate monohydrate (LAT)

(M = 191.07; [D: 201.13])

1a Ferroelectricity in $LiNH_4C_4H_4O_6 \cdot H_2O$ was discovered independently by Matthias et al. and Merz in 1951. 51Mat 51Mer

b

phase	II [a) b)]	I [a) b)]
state	F [a) b)]	P [a) b)]
crystal system	monoclinic [c) d)]	orthorhmbic [c)]
space group	$P12_11 - C_2^2$ [d)]	$P2_12_12 - D_2^3$ [c)]
Θ [K]	106 [b)]	

[a)] 51Mat
[b)] 51Mer
[c)] 53Ver
[d)] 62Jon

Crystal system below Θ_{II-I} was suggested to triclinic instead of monoclinic. 81Jai, 94Glu

P_s || [010]. 51Mat
Transparent, colorless. 89Kor
$\rho = 1.73 \cdot 10^3$ kg m^{-3}, $\rho_X = 1.721 \cdot 10^3$ kg m^{-3} at RT. 56Zhd

2a Crystal growth: evaporation or cooling method from aqueous solution. 72ElS
b Crystal form: Fig. 68A-1-001.

3a Unit cell parameters: a = 7.884(6) Å, b = 14.565(8) Å, c = 6.409(4) Å at RT. 72Hin
b Structure of phase I: Z = 4. 53Ver, 72Hin

Fractional coordinates: Table 68A-1-001.
Temperature parameters: Table 68A-1-002.
Fractional coordinates of hydrogens and their temperature parameters: Table 68A-1-003.
Interatomic distances and bond angles: Table 68A-1-004.
Schematic drawing of the tartrate molecule: Fig. 68A-1-002.
The structure projected onto (001) and (100): Fig. 68A-1-003, Fig. 68A-1-004.

4 Spontaneous shear strain below Θ_{II-I}: spontaneous strain $S_6 \approx 0.021$ at 70.5 K. 78Ter

5a Dielectric constant: Fig. 68A-1-005, Fig. 68A-1-006.
$\kappa_{22}^{\mathbf{T}}$ shows a large anomaly around Θ_{II-I} = 98 K, but $\kappa_{22}^{\mathbf{S}}$ reveals no anomaly: Fig. 68A-1-007. 77Saw
c Spontaneous polarization and coercive field: $P_s = 0.22 \cdot 10^{-2}$ C m^{-2} at 78 K, 51Mat
$E_c \approx 1 \cdot 10^{-6}$ V m^{-1} at 78 K.
See also 51Mer, 94Glu

6a Heat capacity: Fig. 68A-1-008.

7a Piezoelectric constant $d_{i\lambda}$: Fig. 68A-1-009.

8a Elastic compliance: Fig. 68A-1-010, Fig. 68A-1-011.
Elastic stiffness $c_{55}^{\boldsymbol{E}}$ and $c_{55}^{\boldsymbol{P}}$: Fig. 68A-1-012.

	Elastic stiffness obtained from Brillouin scattering: Fig. 68A-1-013.	
9a	Refractive indices: $n_a = 1.5580$, $n_b = 1.5773$, $n_c = 1.5216$ at $\lambda = 632.8$ nm.	89Kor
	See also	78Uda
	Biaxial positive.	89Kor
	Optical axes lie in (001), $2V = 87.8°$ at RT.	89Kor
	Spontaneous birefringence: see	84Iva
	Rotation of optical indicatrix: Fig. 68A-1-014.	
	Infrared reflectivity and transmission spectra: see	96Kam
d	Optical rotatory power: Fig. 68A-1-015, Fig. 68A-1-016.	
10a	Raman scattering: see	79Uda, 96Kam
b	Brillouin scattering: see	77Saw, 78Uda
13a	Deuteron quadrupole coupling tensor in deuterated crystal: Table 68A-1-005, Table 68A-1-006.	
	^7Li quadrupole coupling tensor, asymmetry parameter: Table 68A-1-007.	
b	Spin Hamiltonian parameters for Mn^{2+}: Table 68A-1-008.	
	See also	76Nav
	Spin Hamiltonian parameters for Cr^{3+}: Table 68A-1-009.	
15a	Four kinds of domains were found in ESR study.	81Jai
	Light deflection and diffraction at domain walls: see	89Kor, 92Sza
	Striped domains were observed in phase II by polarized light.	89Kor

Table 68A-1-001. $LiNH_4C_4H_4O_6 \cdot H_2O$ (LAT). Structure of phase I [72Hin]. Fractional coordinates at RT. O(W): oxygen of water molecule, see Fig. 68A-1-003.

	x	*y*	*z*
O(1)	0.2176(2)	0.1260(1)	0.1878(2)
O(2)	0.3134(2)	0.2113(1)	–0.0762(2)
O(3)	0.3736(2)	0.4384(1)	0.6018(3)
O(4)	0.1218(2)	0.3692(1)	0.6210(3)
O(5)	0.2355(2)	0.3662(1)	0.0947(2)
O(6)	0.5046(2)	0.3163(1)	0.3564(2)
O(W)	0.3265(2)	0.0731(2)	0.6483(3)
N(1)	0.0000	0.0000	–0.0534(5)
N(2)	0.0000	0.5000	–0.0842(5)
C(1)	0.2527(2)	0.2011(1)	0.1027(3)
C(2)	0.2127(2)	0.2885(1)	0.2255(2)
C(3)	0.3342(2)	0.2984(1)	0.4147(2)
C(4)	0.2717(2)	0.3756(1)	0.5560(3)
Li	0.1266(5)	0.0780(1)	0.4501(6)

Table 68A-1-002. $LiNH_4C_4H_4O_6 \cdot H_2O$ (LAT). Structure of phase I [72Hin]. Temperature parameters at RT. b_{ij} is defined by Eq. (b) in Introduction. See also Fig. 68A-1-003.

	b_{11}	b_{22}	b_{33}	b_{12}	b_{13}	b_{23}
	10^{-4}					
O(1)	89(2)	14(1)	105(3)	–6(1)	13(2)	–2(1)
O(2)	129(3)	23(1)	86(3)	–9(1)	40(2)	–9(1)
O(3)	61(2)	14(1)	182(4)	–3(1)	–12(2)	–19(1)
O(4)	67(2)	29(1)	147(3)	–8(1)	45(2)	–27(1)
O(5)	116(2)	14(1)	93(3)	3(1)	–28(2)	6(1)
O(6)	36(1)	28(1)	135(3)	3(1)	5(2)	–11(1)
O(W)	93(2)	24(1)	148(4)	2(1)	–13(3)	–15(1)
N(1)	93(4)	26(1)	132(6)	6(2)	0	0
N(2)	82(3)	21(1)	162(6)	7(2)	0	0
C(1)	49(2)	14(1)	72(3)	–3(1)	0(2)	–6(1)
C(2)	46(2)	12(1)	72(3)	2(1)	–5(2)	–3(1)
C(3)	43(2)	11(1)	69(3)	1(1)	1(2)	–1(1)
C(4)	54(2)	12(1)	78(3)	0(1)	–1(2)	–6(1)
Li	68(5)	19(1)	112(7)	–5(2)	6(5)	6(3)

Table 68A-1-003. $LiNH_4C_4H_4O_6 \cdot H_2O$ (LAT). Structure of phase I [72Hin]. Fractional coordinates of hydrogen atoms and their isotropic temperature parameters at RT. Temperature parameter B is defined by Eq. (e) in Introduction. See also Fig. 68A-1-003.

	x	y	z	B [Å^2]	Bonded to
H(1)	0.059(4)	–0.034(2)	–0.139(5)	2.5(7)	N(1)
H(2)	0.075(4)	0.037(2)	0.027(6)	3.2(9)	N(1)
H(3)	0.066(6)	0.462(3)	–0.032(7)	6.6(16)	N(2)
H(4)	0.078(7)	0.530(4)	–0.190(8)	9.9(18)	N(2)
H(5)	0.320(5)	0.112(3)	0.746(6)	6.2(10)	O(W)
H(6)	0.409(5)	0.074(2)	0.581(6)	6.2(7)	O(W)
H(7)	0.284(4)	0.342(2)	–0.013(6)	4.3(9)	O(5)
H(8)	0.552(4)	0.259(2)	0.346(4)	2.4(6)	O(6)
H(9)	0.095(3)	0.288(2)	0.262(4)	1.2(4)	C(2)
H(10)	0.327(3)	0.238(2)	0.488(4)	1.2(5)	C(3)

Table 68A-1-004. $LiNH_4C_4H_4O_6 \cdot H_2O$ (LAT). Structure of phase I [72Hin]. Interatomic distances and angles related to hydrogen atoms at RT. e.s.d.: estimated standard deviation. See also Fig. 68A-1-003.

Distance	[Å]	Angle	[deg]
N(1)–H(1)	0.90	C(2)–O(5)–H(7)	102
N(1)–H(2)	0.91	C(3)–O(6)–H(8)	105
N(2)–H(3)	0.83		
N(2)–H(4)	1.01	C(1)–C(2)–H(9)	107
O(W)–H(5)	0.87	C(3)–C(2)–H(9)	113
O(W)–H(6)	0.87	O(5)–C(2)–H(9)	104
O(5)–H(7)	0.88	C(2)–C(3)–H(10)	105
O(6)–H(8)	0.89	C(4)–C(3)–H(10)	110
C(2)–H(9)	0.99	O(6)–C(3)–H(10)	111
C(3)–H(10)	0.99	⟨e.s.d.⟩ =	1.6
⟨e.s.d.⟩ =	0.04		

Table 68A-1-005. Deuterated LAT. Eigenvalues and transformation matrix of deuteron quadrupole coupling tensor of D_2O [72ElS]. T = 330 K. (*1*, *2*, *3*) are the principal axes of the tensor, (*a*, *b*, *c*) are the crystallographic axes.

	$eq\phi_{xx}/h$	$eq\phi_{yy}/h$	$eq\phi_{zz}/h$
Eigenvalues [kHz]	–14	–102	116

	a	*b*	*c*
1	–0.678	0.702	0.217
2	–0.395	–0.597	0.699
3	0.620	0.388	0.682

e^2qQ/h = 116 kHz; η = 0.761

Table 68A-1-006. Deuterated LAT. Eigenvalues and transformation matrix of deuteron quadrupole coupling tensor of ND_4^+ [72ElS]. (*1*, *2*, *3*) are the principal axes of the tensor, (*a*, *b*, *c*) are the crystallographic axes.

$T = 111$ K	$eq\phi_{xx}/h$	$eq\phi_{yy}/h$	$eq\phi_{zz}/h$
Eigenvalues [kHz]	–2.3	–3.3	5.6
	a	*b*	*c*
1	0.09	–0.07	0.99
2	0.71	–0.69	–0.11
3	0.69	0.71	–0.03

$T = 77$ K	$eq\phi_{xx}/h$	$eq\phi_{yy}/h$	$eq\phi_{zz}/h$
Eigenvalues [kHz]	–0.5	–3.9	4.4
	a	*b*	*c*
1	0.69	–0.43	0.58
2	–0.56	0.18	0.81
3	0.45	0.88	0.12

Table 68A-1-007. $LiNH_4C_4H_4O_6 \cdot H_2O$ (LAT). ^7Li quadrupole coupling tensor, asymmetry parameter η, and orientation of the principal axes (*1*, *2*, *3*) of the electric field gradient tensor with respect to the crystallographic axes (*a*, *b*, *c*) [72ElS]. $T = 300$ K.

	$eq\phi_{xx}/h$	$eq\phi_{yy}/h$	$eq\phi_{zz}/h$
Eigenvalues [kHz]	–33.0	–44.6	77.6
	a	*b*	*c*
1	0.135	0.797	–0.604
2	0.267	0.579	0.770
3	0.964	–0.172	–0.205

$e^2qQ/h = 77.6$ kHz; $\eta = 0.150$

Table 68A-1-008. $LiNH_4C_4H_4O_6{\cdot}H_2O{:}Mn^{2+}$. Spin Hamiltonian parameter of Mn^{2+} [81Jai]. $T \approx 300$ K.

D	$4.85(2) \cdot 10^4$ A m^{-1}
E	$-8.67(16) \cdot 10^3$ A m^{-1}
b_{40}	$1.43(2) \cdot 10^2$ A m^{-1}
b_{42}	$2.39(4) \cdot 10^3$ A m^{-1}
b_{44}	not certain
g_x	2.010(4)
g_y	2.005(4)
g_z	2.007(2)
A_x	$-7.28(4) \cdot 10^3$ A m^{-1}
A_y	$-7.16(8) \cdot 10^3$ A m^{-1}
A_z	$-7.00(4) \cdot 10^3$ A m^{-1}

Table 68A-1-009. $LiNH_4C_4H_4O_6 \cdot H_2O:Cr^{3+}$. The principal values of *D*-tensor and their direction cosines with respect to the *a*, *b*, *c* axes for A-sites and B-sites [75Mae]. *D*: fine structure parameter.

	The principal value		*l*	*m*	*n*
A-site	D_{zz}	$-25.59 \cdot 10^{-1}$ m^{-1}	0.238	–0.283	0.929
	D_{yy}	$15.80 \cdot 10^{-1}$ m^{-1}	–0.021	0.955	0.296
	D_{xx}	$9.79 \cdot 10^{-1}$ m^{-1}	0.971	0.091	–0.221
B-site	D_{zz}	$31.69 \cdot 10^{-1}$ m^{-1}	0.868	–0.135	0.479
	D_{yy}	$-21.81 \cdot 10^{-1}$ m^{-1}	0.242	0.956	–0.168
	D_{xx}	$-9.86 \cdot 10^{-1}$ m^{-1}	–0.435	0.262	0.862

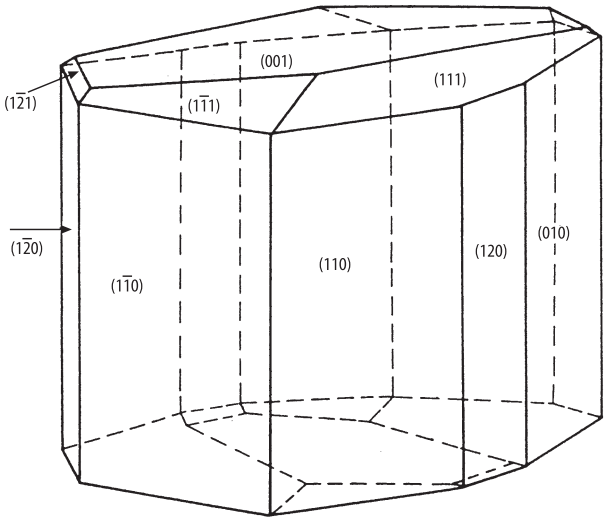

Fig. 68A-1-001. $LiNH_4C_4H_4O_6 \cdot H_2O$ (LAT). Crystal form [89Kor].

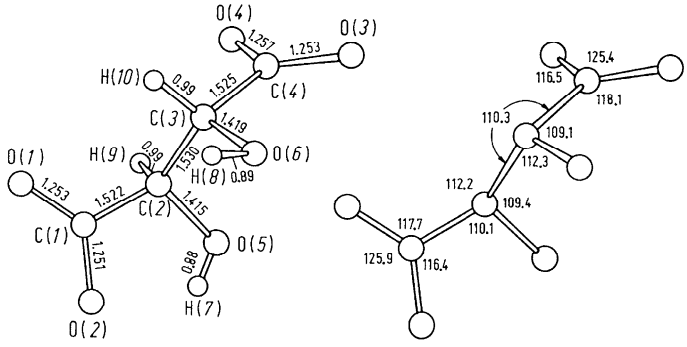

Fig. 68A-1-002. $LiNH_4C_4H_4O_6 \cdot H_2O$ (LAT). Structure of phase I [72Hin]. Schematic view showing tartrate molecule. Bond lengths [Å] and angles [°] are shown in the left and right figures, respectively.

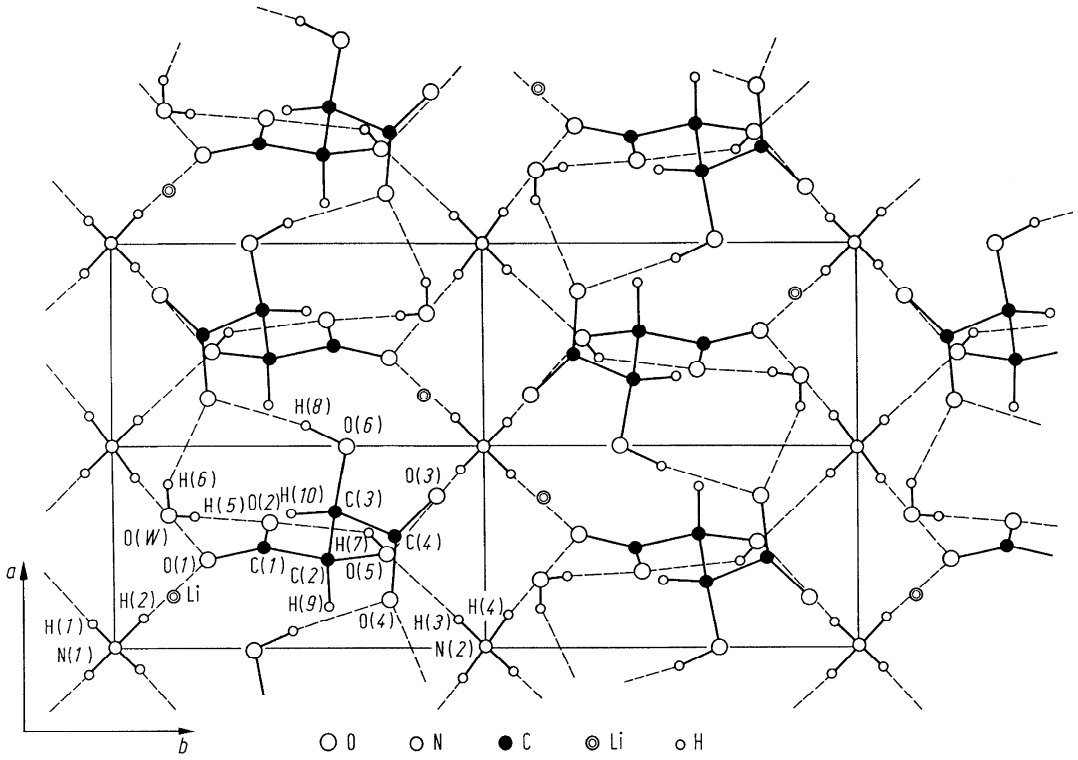

Fig. 68A-1-003. $LiNH_4C_4H_4O_6 \cdot H_2O$ (LAT). Structure of phase I [72Hin]. Projection onto (001). The hydrogen bonds are shown by broken lines.

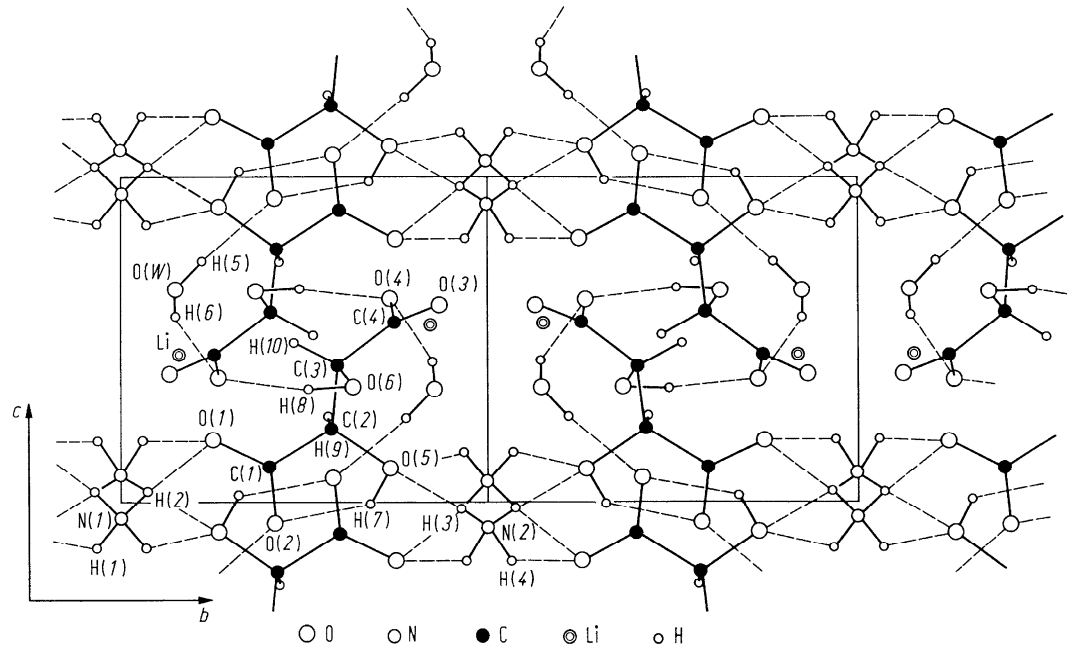

Fig. 68A-1-004. $LiNH_4C_4H_4O_6 \cdot H_2O$ (LAT). Structure of phase I [72Hin]. Projection onto (100). The broken lines represent hydrogen bonds.

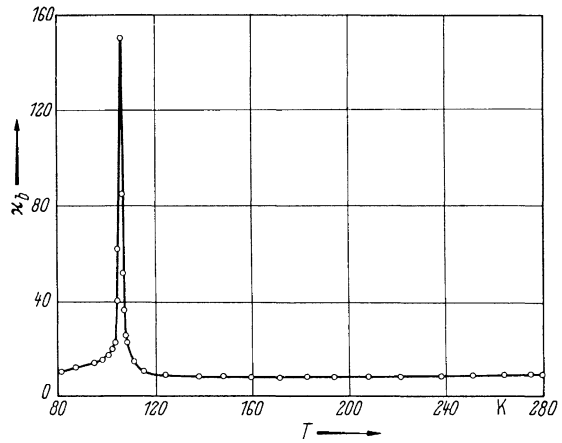

Fig. 68A-1-005. $LiNH_4C_4H_4O_6 \cdot H_2O$ (LAT). κ_b vs. T [51Mer].

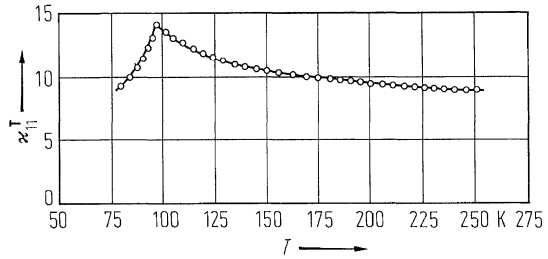

Fig. 68A-1-006. $LiNH_4C_4H_4O_6 \cdot H_2O$ (LAT). $\kappa_{11}^{\mathbf{T}}$ vs. T [77Mae]. $f = 1$ kHz.

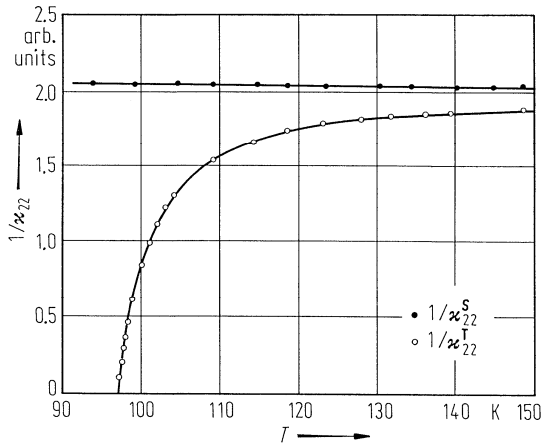

Fig. 68A-1-007. $LiNH_4C_4H_4O_6 \cdot H_2O$ (LAT). $1/\kappa_{22}^{\mathbf{S}}$, $1/\kappa_{22}^{\mathbf{T}}$ vs. T [77Saw]. $\kappa_{22}^{\mathbf{S}}$: $f = 2$ MHz, $\kappa_{22}^{\mathbf{T}}$: $f = 2$ kHz.

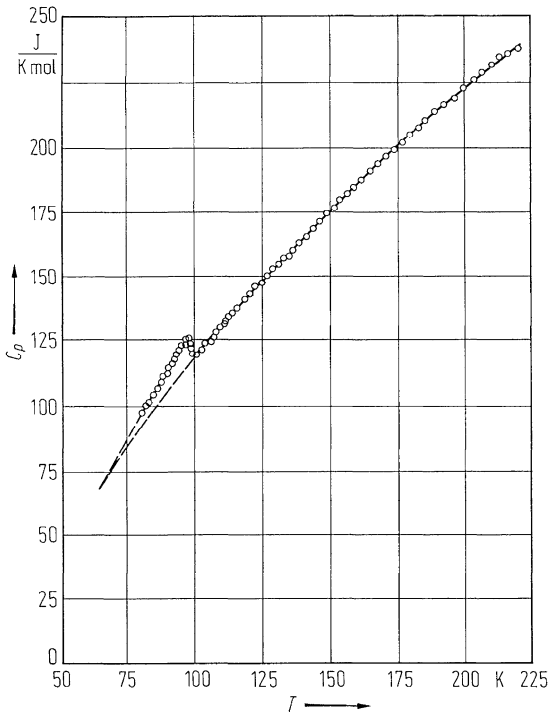

Fig. 68A-1-008. $LiNH_4C_4H_4O_6 \cdot H_2O$ (LAT). C_p vs. T [73Mak]. C_p: molar heat capacity at constant pressure.

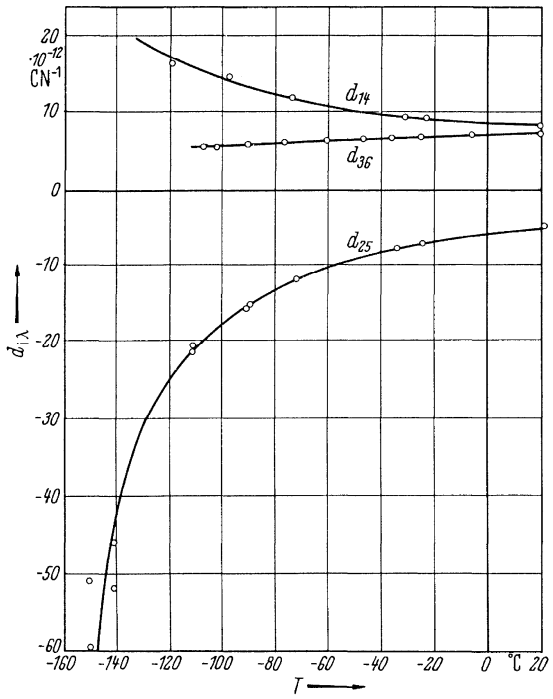

Fig. 68A-1-009. $LiNH_4C_4H_4O_6 \cdot H_2O$ (LAT). $d_{i\lambda}$ vs. T [66Bec].

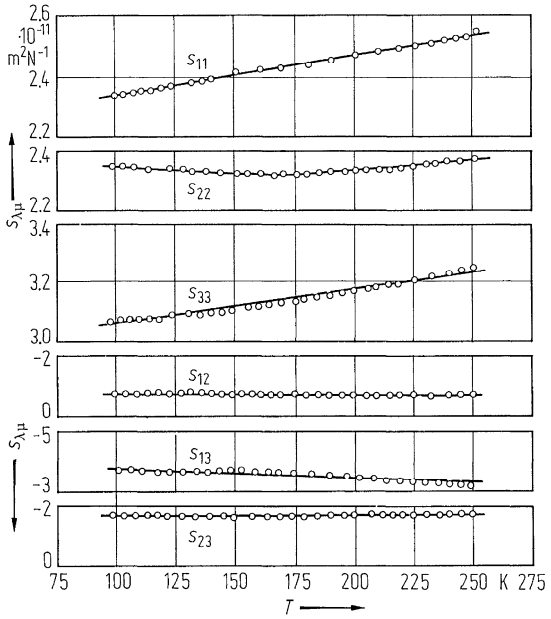

Fig. 68A-1-010. $LiNH_4C_4H_4O_6 \cdot H_2O$ (LAT). $s_{\lambda\mu}$ vs. T [77Mae].

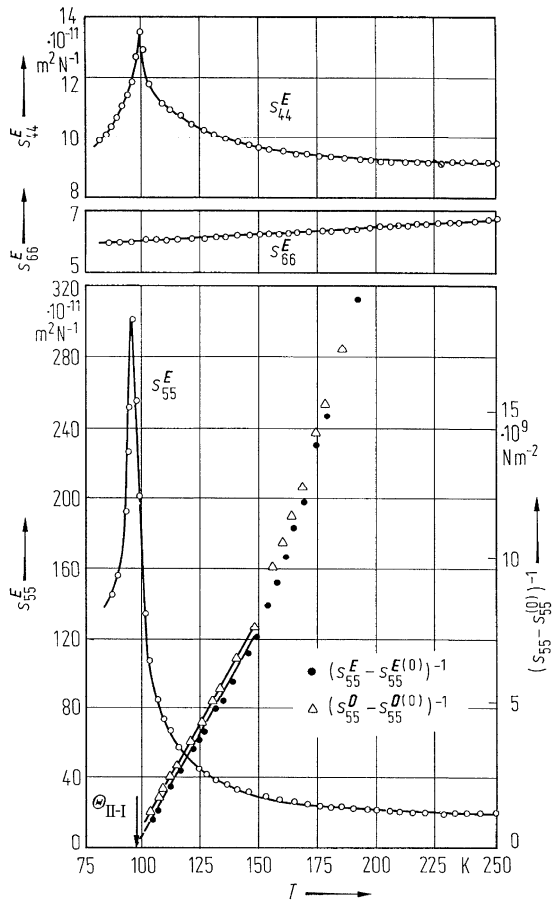

Fig. 68A-1-011. $LiNH_4C_4H_4O_6 \cdot H_2O$ (LAT). Elastic compliances (shear components) vs. T [77Mae]. Two straight lines show $(s^E_{55} - s^{E(0)}_{55})^{-1}$ and $(s^D_{55} - s^{D(0)}_{55})^{-1}$, where the values for $s^{E(0)}_{55}$ and $s^{D(0)}_{55}$ are taken as 18.0 and 17.0 · 10^{-11} $m^2 N^{-1}$, respectively.

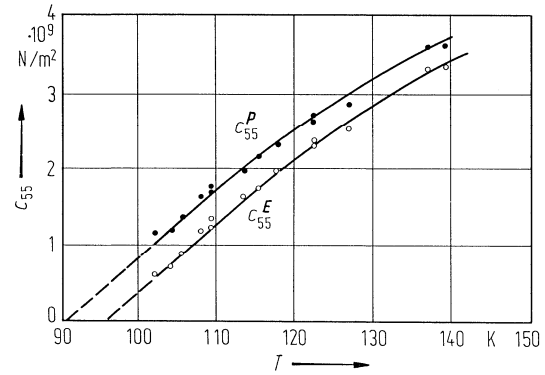

Fig. 68A-1-012. $LiNH_4C_4H_4O_6 \cdot H_2O$ (LAT). c^P_{55}, c^E_{55} vs. T [77Saw].

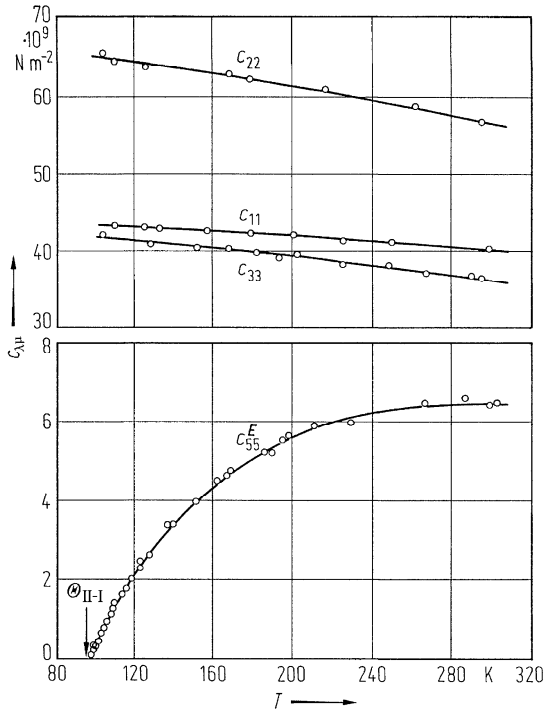

Fig. 68A-1-013. $LiNH_4C_4H_4O_6 \cdot H_2O$ (LAT). $c_{\lambda\mu}$ vs. T [78Uda]. $c_{\lambda\mu}$: elastic stiffness constant obtained from Brillouin scattering.

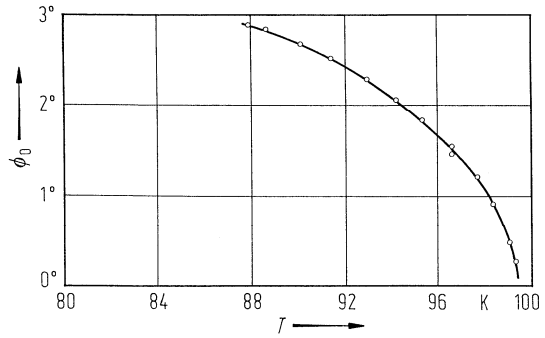

Fig. 68A-1-014. $LiNH_4C_4H_4O_6 \cdot H_2O$ (LAT). ϕ_0 vs. T [84Iva]. ϕ_0: rotation angle of the optical indicatrix below Θ_{II-I}. $\lambda = 633$ nm.

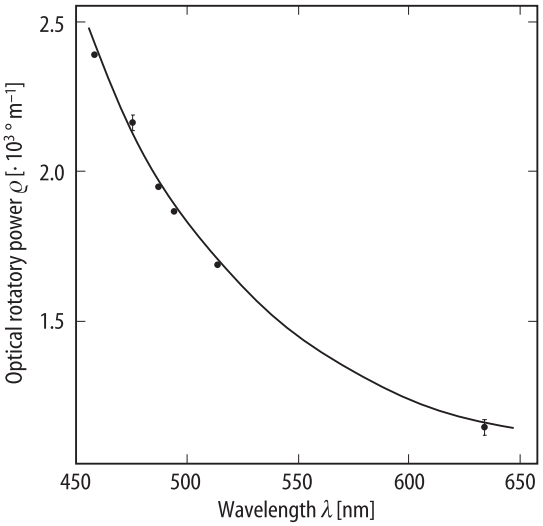

Fig. 68A-1-015. $LiNH_4C_4H_4O_6 \cdot H_2O$ (LAT). ρ vs. λ [89Kor]. ρ: optical rotatory power along the optical axis. T = 293 K.

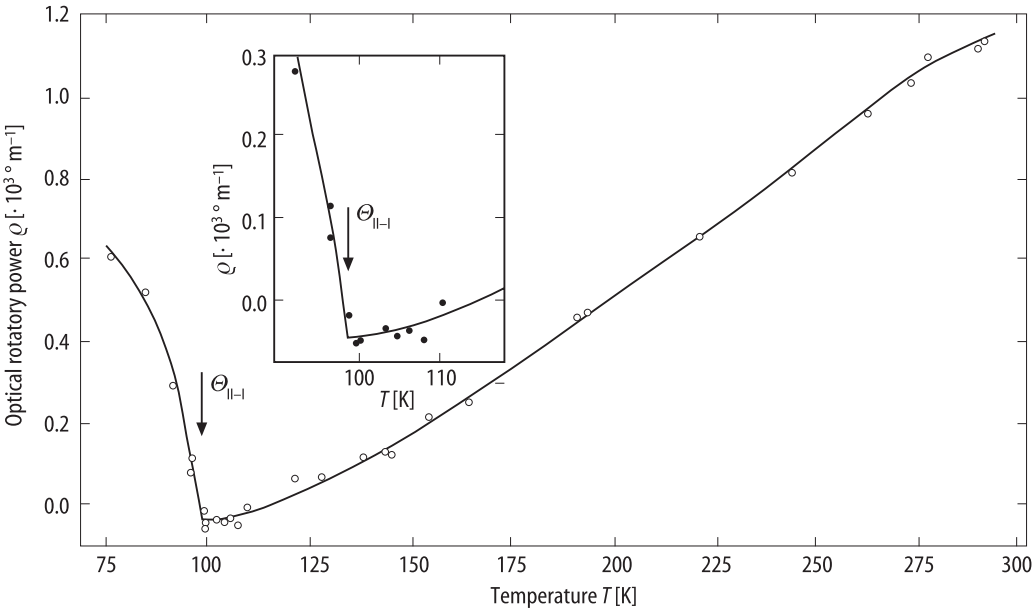

Fig. 68A-1-016. $LiNH_4C_4H_4O_6 \cdot H_2O$ (LAT). ρ vs. T [89Kor]. ρ: optical rotatory power along the optical axis. λ = 632.8 nm.

References

51Mat Matthias, B.T., Hulm, J.K.: Phys. Rev. **82** (1951) 108.
51Mer Merz, W.J.: Phys. Rev. **82** (1951) 562; erratum **83** (1951) 656.
53Ver Vernon, R.C., Pepinsky, R.: Unpublished work (1953), cited in [62Bur].
56Zhd Zhdanov, G.S., Umanskii, M.M., Varfolomeeva, L.A., Ezhkova, Z.I., Zolina, Z.K.: Kristallografiya **1** (1956) 271; Sov. Phys. Crystallogr. (English Transl.) **1** (1956) 210.
62Bur Burns, G.: Phys. Rev. **127** (1962) 1193.
62Jon Jona, F., Shirane, G.: Ferroelectric Crystals, Oxford: Pergamon Press, 1962.
66Bec Bechmann, R., Hearmon, R.F.S.: Landolt-Börnstein, New Series, Group III, Vol. 1: Elastic, Piezoelectric, Piezooptic and Electrooptic Constants of Crystals, Hellwege, K.-H., Hellwege, A.M. (eds.), Berlin, Heidelberg, New York: Springer, 1966.
72ElS El Saffar, Z.M., O'Reilly, D.E., Peterson, E.M., Flick, C.: J. Chem. Phys. **57** (1972) 2372.
72Hin Hinazumi, H., Mitsui, T.: Acta Crystallogr. Sect. B **28** (1972) 3299.
73Mak Makita, Y., Wada, K.: J. Phys. Soc. Jpn. **34** (1973) 1111.
75Mae Maeda, M., Suzuki, I., Abe, R.: J. Phys. Soc. Jpn. **39** (1975) 1319.
76Nav Navalgund, R., Gupta, L.C.: Solid State Commun. **19** (1976) 1205.
77Mae Maeda, M., Ikeda, T.: J. Phys. Soc. Jpn. **42** (1977) 1931.
77Saw Sawada, A., Udagawa, M., Nakamura, T.: Phys. Rev. Lett. **39** (1977) 829; erratum **39** (1977) 902.
78Ter Terauchi, H., Takenaka, H., Matsumori, N., Sawada, A.: J. Phys. Soc. Jpn. **44** (1978) 1751.
78Uda Udagawa, M., Kohn, K., Nakamura, T.: J. Phys. Soc. Jpn. **44** (1978) 1873.
79Uda Udagawa, M., Tominaga, Y., Kohn, K., Nakamura, T., Maeda, M.: J. Phys. Soc. Jpn. **47** (1979) 869.
81Jai Jain, A.K., Upreti, G.C.: J. Chem. Phys. **75** (1981) 1623.
84Iva Ivanov, N.R.: Ferroelectrics Lett. **2** (1984) 45.
89Kor Koralewski, M., Szafranski, M.: Ferroelectrics **97** (1989) 233.
92Sza Szafranski, M.: Ferroelectrics **129** (1992) 55.
94Glu Glushkov, V.F., Magataev, V.K., Gladkii, V.V.: Fiz. Tverd. Tela **36** (1994) 1311; Sov. Phys. Solid State (English Transl.) **36** (1994) 716.
96Kam Kamba, S., Brezina, B., Petzelt, J., Schaack, G.: J. Phys. Condens. Matter **8** (1996) 8669.

No. 68A-2 $LiTlC_4H_4O_6 \cdot H_2O$, Lithium thallium tartrate monohydrate (LTT)

(M = 377.41; [D: 383.45])

1a	Ferroelectricity in $LiTlC_4H_4O_6 \cdot H_2O$ was discovered by Matthias et al. in 1951.			51Mat
b	phase	II [a])	I [a])	[a]) 51Mat
	state	F [a])	P [a])	[b]) 62Jon
	crystal system		orthorhombic [b])	
	space group		$P2_12_12 - D_2^3$ [b])	
	Θ [K]	11.6 [c])		[c]) 96Kam
	P_s || [100].			51Mat
	$\rho_X = 3.38 \cdot 10^3$ kg m^{-3}.			71McC
	Transparent, colorless.			70Bre
2a	Cooling method from aqueous solution.			70Bre
	Solubility coefficient: 0.5 g °C^{-1} per 100 g solvent in 10…50 °C range.			70Bre
	Crystal form: Fig. 68A-2-001.			
3a	Unit cell parameters: a = 7.894(3) Å, b = 14.658(6) Å, c = 6.401(3) Å at 20 °C.			71McC
	Deuterated crystal (more than 80 % of H is replaced by D), a = 7.91(1) Å, b = 14.69(6) Å, c = 6.43(4) Å.			70Bre
b	Z = 4 in phase I.			55Shi, 71McC
	Fractional coordinates and temperature parameters: Table 68A-2-001.			
	Interatomic distances and bond angles: Table 68A-2-002.			
	The structure projected onto (001): Fig. 68A-2-002.			
5a, b	Dielectric constant: Fig. 68A-2-003, Fig. 68A-2-004, Fig. 68A-2-005, Fig. 68A-2-006, Fig. 68A-2-007.			
	Curie-Weiss law: $\kappa_a = \kappa_\infty + C/(T - \Theta_p)$, $T > \approx 15$ K, with κ_∞ = 9, C = 1330 K, Θ_p = 11 K for free crystal (low frequency, $\kappa_a^{\mathbf{T}}$); κ_∞ = 9, C = 1500 K, Θ_p = –50 K for clamped crystal (high frequency, $\kappa_a^{\mathbf{S}}$).			72Saw
	κ_a vs. measuring field (1 kHz, 10^{-1}…10^4 V m^{-1}) at 4.2 K: see			71Saw1
	Dielectric constant in the submillimeter range: Fig. 68A-2-008.			
	Effect of dc field on κ_a: Fig. 68A-2-009.			
	κ_a^{-1} vs. T at various hydrostatic pressures: Fig. 68A-2-010; see also			96Kam
	Θ_p vs. p: Fig. 68A-2-011; $(d\Theta_p/dp)_{p=0} = 11.3 \cdot 10^{-8}$ K Pa^{-1}.			70Heg
	Θ_{II-I} vs. p: Fig. 68A-2-012; $\Theta_{II-I}(p) = \Theta_{II-I}(0) + Ap^{1/2}$, with $\Theta_{II-I}(0)$ = 11.6 K and $A = 6.89 \cdot 10^{-2}$ K Pa$^{-1/2}$.			96Kam
c	Spontaneous polarization and coercive field: Fig. 68A-2-013; see also			82Nov, 93Deg
6a	Heat capacity below ≈20 K: Fig. 68A-2-014.			
b	Thermal conductivity below ≈80 K; a large anisotropy was observed, $\lambda_a/\lambda_b \approx 10$.			78Heg
	For deuterated crystal: see			80Heg
7a	Piezoelectric constant d_{14}: Fig. 68A-2-015.			
	Electromechanical coupling factor: Fig. 68A-2-016.			

8a	Elastic compliances and stiffnesses: Fig. 68A-2-017, Fig. 68A-2-018. Effects of dc field on elastic compliances: Fig. 68A-2-019.	
9a	Optical and electro-optical properties: see Far infrared spectrum: see	86Zhu 96Kam
10a	Raman scattering: Fig. 68A-2-020; see also	88Kha
b	Brillouin scattering: see	88Pav
13a	NMR: see	62Bur
b	ESR: $\boldsymbol{g}$ and $\boldsymbol{A}$ tensors for Tl^{2+} centers: Table 68A-2-003.	

Table 68A-2-001. $LiTlC_4H_4O_6 \cdot H_2O$ (LTT). Structure of phase I [78Kay]. Neutron diffraction. (a): fractional coordinates, (b): temperature parameters b_{ij}. The b_{ij} is defined by Eq. (b) in Introduction. See also Fig. 68A-2-002.

Atom		(a) Fractional coordinates			(b) Temperature parameters					
		X	*Y*	*Z*	b_{11}	b_{22}	b_{33}	b_{12}	b_{13}	b_{23}
Carbon	1	0.2551(2)	0.2010(1)	0.0998(3)	75(4)	14.1(10)	139(5)	–3(1)	8(4)	–5(2)
	2	0.2188(3)	0.2887(1)	0.2215(3)	52(4)	17.3(10)	141(5)	1(2)	–5(4)	–9(2)
	3	0.3342(2)	0.2994(1)	0.4124(3)	54(3)	16.9(10)	116(5)	–2(1)	1(3)	–9(2)
	4	0.2724(3)	0.3768(1)	0.5549(3)	61(4)	16.9(10)	142(6)	0(2)	3(4)	–9(2)
Oxygen	1	0.2214(4)	0.1265(2)	0.1896(4)	127(5)	15.5(11)	152(6)	0(2)	11(5)	–4(2)
	2	0.3160(4)	0.2102(2)	–0.0766(4)	170(6)	23.8(12)	139(7)	–14(2)	50(5)	–8(2)
	3	0.3744(3)	0.4375(2)	0.6066(4)	64(4)	16.8(10)	235(8)	–4(2)	–39(5)	–24(2)
	4	0.1212(3)	0.3709(2)	0.6141(5)	66(5)	41.3(14)	226(7)	–9(2)	34(6)	–40(3)
	5	0.2379(4)	0.3645(2)	0.0878(5)	152(6)	15.9(12)	166(9)	6(2)	–31(5)	4(3)
	6	0.5054(3)	0.3159(2)	0.3559(4)	38(4)	39.1(15)	205(8)	6(2)	–15(6)	–20(3)
	W [a])	0.3253(5)	0.0737(2)	0.6428(5)	136(7)	24.2(13)	153(6)	15(3)	–43(6)	–4(3)
Hydrogen	W 1	0.3277(6)	0.1221(4)	0.7498(8)	176(11)	34.7(22)	153(12)	13(4)	8(9)	–14(5)
	W 2	0.4307(8)	0.0809(4)	0.5751(12)	121(9)	65.4(39)	354(20)	10(5)	–13(13)	–35(8)
	1	0.2665(10)	0.3393(4)	–0.0455(9)	431(19)	33.4(24)	148(14)	–24(6)	52(15)	–2(5)
	2	0.5583(7)	0.2607(5)	0.3283(10)	94(9)	61.7(40)	384(20)	11(5)	–15(9)	–87(8)
	3	0.0875(6)	0.2836(3)	0.2761(7)	86(9)	50.8(25)	201(12)	7(4)	13(9)	–29(5)
	4	0.3258(6)	0.2366(3)	0.4997(8)	160(8)	24.5(21)	214(12)	0(3)	–16(9)	2(4)
Lithium		0.1220(9)	0.0803(5)	0.4437(11)	54(11)	46.9(40)	166(18)	–20(6)	–6(12)	10(8)
Thallium	1	0.0	0.0	0.9521(5)	123(4)	43.7(13)	200(7)	3(2)	–	–
	2	0.0	0.5	0.9109(4)	90(4)	31.9(11)	181(7)	–5(2)	–	–

Table 68A-2-002. $LiTlC_4H_4O_6 \cdot H_2O$ (LTT). Structure of phase I [78Kay]. Neutron diffraction. Interatomic distances and angles. Values corrected for "riding motion" are presented in square brackets. Primes are attached to atoms to remark that the atoms are symmetry related to those without primes. See also Fig. 68A-2-002.

1. Tartrate ion

Atoms	Distance [Å] or angle [°]
a) Carbon skeleton	
C(1)–C(2)	1.528(6)
C(2)–C(3)	1.531(6)
C(3)–C(4)	2.534(5)
C(1)–C(2)–C(3)	112.4(2)
C(2)–C(3)–C(4)	111.2(3)
b) Carboxyl groups	
O(1)–C(1)	1.260(6)
O(2)–C(1)	1.234(6)
O(1)–C(1)–O(2)	126.4(3)
O(1)–C(1)–C(2)	117.0(4)
O(2)–C(1)–C(2)	116.6(3)
O(3)–C(4)	1.242(5)
O(4)–C(4)	1.253(7)
O(3)–C(4)–O(4)	125.7(3)
O(3)–C(4)–C(3)	118.7(3)
O(4)–C(4)–C(3)	115.5(2)
c) Hydroxyl groups and methyl hydrogen atoms	
C(2)–O(5)	1.409(6)
O(5)–H(1)	0.956 [1.012] (9)
C(2)–H(3)	1.095 [1.118] (8)
H(1)–O(5)–C(2)	105.3(5)
O(5)–C(2)–H(3)	110.4(3)
O(5)–C(2)–C(1)	109.3(4)
H(3)–C(2)–C(1)	106.3(3)
C(3)–O(6)	1.418(7)
O(6)–H(2)	0.925 [0.962] (10)
C(3)–H(4)	1.076 [1.102] (7)
H(2)–O(6)–C(3)	109.2(5)
O(6)–C(3)–H(4)	109.6(3)
O(6)–C(3)–C(4)	109.1(3)
H(4)–C(3)–C(4)	107.6(4)
O(6)–C(3)–C(2)	112.3(3)
O(5)–C(2)–C(3)	109.9(3)
H(4)–C(3)–C(2)	106.9(3)
H(3)–C(2)–C(3)	108.3(4)

2. Lithium coordination (distorted quadrilateral pyramid)

Atoms	Distance [Å] or angle [°]	
Li–O(1)	1.928(10)	
Li–O(3)	1.995(11)	
Li–O(3)'	2.114(12)	
Li–OW	2.049(11)	
Li–O(6)	2.190(10)	
O(1)–Li–O(3)	107.9(4)	
O(1)–Li–O(3)'	102.3(4)	
O(1)–Li–OW	102.9(5)	
O(1)–Li–O(6)	114.9(5)	
O(3)–Li–O(3)'	82.0(2)	
O(3)–Li–O(6)	76.9(3)	
O(3)'–Li–OW	92.2(3)	
OW–Li–O(6)	89.8(4)	
O(3)'–Li–O(6)	141.3(4)	
O(3)–Li–OW	149.2(4)	
O(3)–O(3)'	2.696(10)	
O(3)'–OW	2.999(9)	
OW–O(6)	2.994(12)	
O(6)–O(3)	2.608(9)	
O(3)–O(3)'–OW	86.2(4)	$\Sigma = 359.3$
O(3)'–OW–O(6)	85.3(3)	
OW–O(6)–O(3)	87.9(3)	
O(6)–O(3)–O(3)'	99.9(3)	

(continued)

Table 68A-2-002 (continued)

3. Thallium coordination

Thallium is on a two-fold axis and all oxygen atoms listed have related atoms equidistant from Tl (OJ and OJ').

Atoms	Distance [Å] or angle [°]	Atoms	Distance [Å] or angle [°]
a) Thallium 1		b) Thallium 2	
Tl(1)–O(5)	2.874(10)	Tl(2)–O(4)	2.845(9)
Tl(1)–O(1)	2.963(9)	Tl(2)–O(1)	2.943(10)
Tl(1)–O(3)	3.130(13)	Tl(2)–O(5)	2.954(9)
Tl(1)–O(6)	3.338(12)	Tl(2)–OW)	2.349(12)
Tl(1)–OW	3.413(12)	O(4)–Tl(2)–O(4)	96.2(4)
O(5)–Tl(1)–O(5)'	169.8(2)	O(1)–Tl(2)–O(1)	154.8(2)
O(1)–Tl(1)–O(1)'	118.3(3)	O(5)–Tl(2)–O(5)	134.9(3)
O(3)–Tl(1)–O(3)	51.0(3)	OW–Tl(2)–OW'	62.9(3)
O(6)–Tl(1)–O(6)	107.6(4)	O(4)–Tl(2)–O(1)	71.7(3)
OW–Tl(1)–OW	109.1(4)	O(1)'	91.2(3)
O(5)–Tl(1)–O(1)	92.2(4)	O(5)	66.2(3)
O(1)	93.1(4)	O(5)'	156.2(1)
O(3)	69.6(2)	OW	119.6(3)
O(3)'	120.6(1)	OW'	130.2(2)
O(6)	53.1(2)	O(1)–Tl(2)–O(1)	97.8(4)
O(6)'	119.7(2)	O(5)'	91.9(4)
OW	105.7(3)	OW	71.2(2)
OW'	68.1(3)	OW'	134.1(1)
O(1)–Tl(1)–O(3)	62.7(3)	O(4)–Tl(2)–O(1)	73.6(3)
O(3)'	62.2(2)	OW'	68.2(2)
O(6)	78.0(3)		
O(6)'	144.5(2)		
OW	70.0(3)		
OW'	159.5(1)		
O(3)–Tl(1)–O(6)	107.5(3)		
O(6)'	139.9(1)		
OW	132.0(2)		
OW'	112.2(3)		
O(6)–Tl(1)–OW	52.6(2)		
OW'	85.5(2)		

4. Hydrogen bonding and water

Bond	Donor H	H-acceptor	Donor-acceptor	O–H–O angle
OW–HW(1)...O(2)	0.985 [0.997] (9)	1.705(8)	2.687(9)	174.7(5)
OW–HW(2)...O(4)	0.943 [0.986] (11)	2.053(10)	2.967(11)	162.5(5)
O(5)–H(1)...O(2)	0.956 [1.012] (9)	1.939(10)	2.566(10)	121.0(4) (internal bond)
O(6)–H(1)...O(4)	0.925 [0.962] (10)	2.022(12)	2.887(13)	155.0(6)
HW(1)–OW–HW(2)		102.8(5)		

Table 68A-2-003. $LiTlC_4H_4O_6 \cdot H_2O$ (LTT), $LiTl_{0.5}(NH_4)_{0.5}C_4H_4O_6 \cdot H_2O$ (LAT-LTT). ***g*** and ***A*** tensors for Tl^{2+} centers [85Toy]. ESR. $T \approx 90$ K. The data for $LiTl_{0.5}(NH_4)_{0.5}C_4H_4O_6 \cdot H_2O$ are in parentheses. ***A***-value in GHz. The errors in the absolute values of ***g*** and ***A*** are ±0.014 and ±2.0 GHz, respectively. *l*, *m*, *n*: direction cosines of the principal axes.

Parameters				Direction cosine		
				l	*m*	*n*
g_x	1.937	A_x	113.6	0.5	0.866	0
	(1.933)		(118.3)			
g_y	1.937	A_y	113.4	–0.866	0.5	0
	(1.933)		(118.1)			
g_z	1.946	A_z	114.7	0	0	1
	(1.954)		(119.4)	(0	0	1)

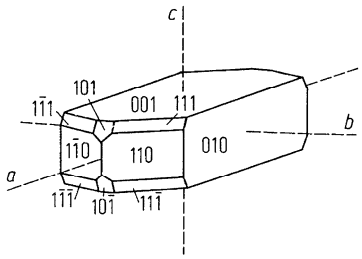

Fig. 68A-2-001. $LiTlC_4H_4O_6 \cdot H_2O$ (LTT). Crystal form [70Bre].

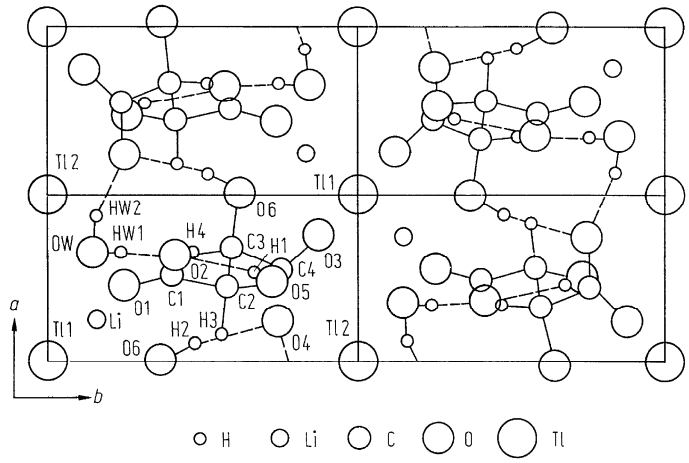

Fig. 68A-2-002. $LiTlC_4H_4O_6 \cdot H_2O$ (LTT). Structure of phase I [78Kay]. Projection onto (001). Neutron diffraction.

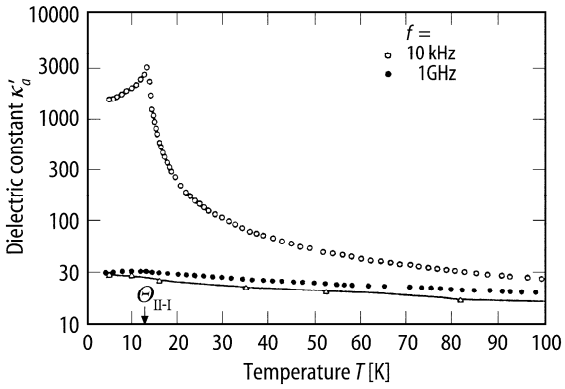

Fig. 68A-2-003. $LiTlC_4H_4O_6 \cdot H_2O$ (LTT). κ'_a vs. T [92Hay]. Parameter: f. Triangles: dielectric constant in submillimeter range [86Vol].

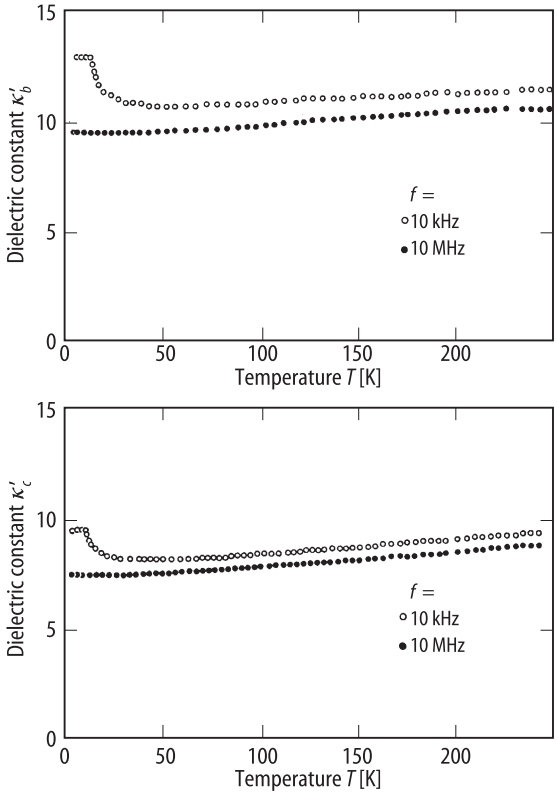

Fig. 68A-2-004. $LiTlC_4H_4O_6 \cdot H_2O$ (LTT). κ'_b, κ'_c vs. T [92Hay]. Parameter: f.

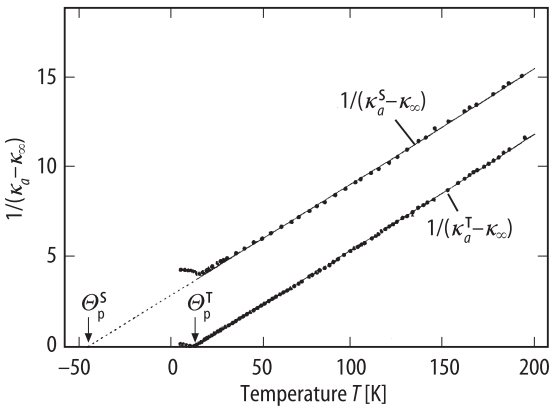

Fig. 68A-2-005. $LiTlC_4H_4O_6 \cdot H_2O$ (LTT). $1/(\kappa_a^T - \kappa_\infty)$, $1/(\kappa_a^S - \kappa_\infty)$ vs. T [92Hay]. κ_a^T: free dielectric constant measured at 10 kHz, κ_a^S: clamped dielectric constant measured at 1 GHz. κ_∞: temperature-independent dielectric constant, $\kappa_\infty = 7.7$.

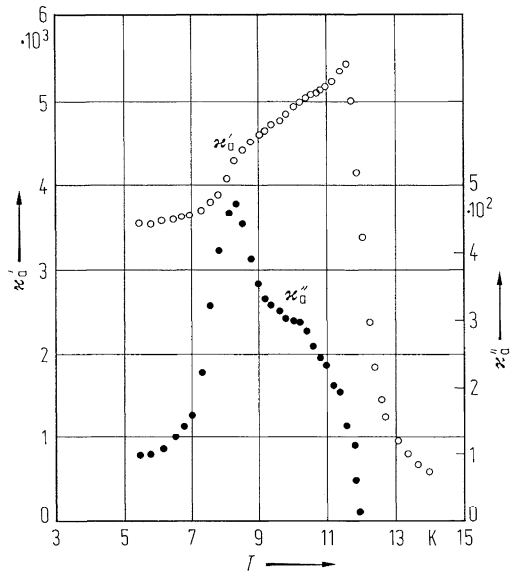

Fig. 68A-2-006. $LiTlC_4H_4O_6 \cdot H_2O$ (LTT). κ'_a, κ''_a vs. T [74Abe]. $f = 1$ kHz.

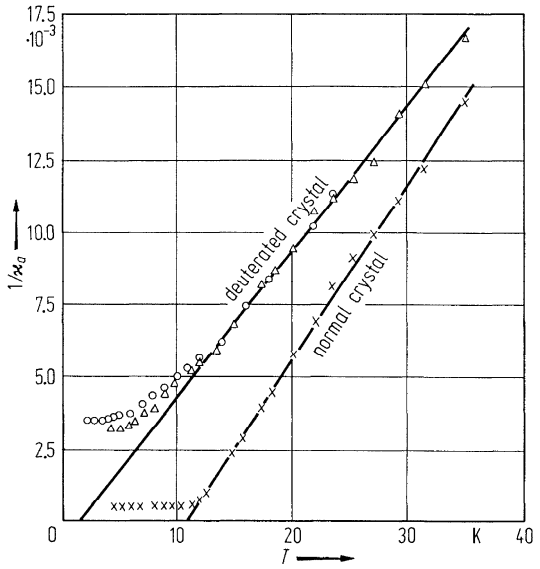

Fig. 68A-2-007. $LiTlC_4H_4O_6 \cdot H_2O$ (LTT). $1/\kappa_a$ vs. T for normal crystal and deuterated crystal (more than 80 % of hydrogen is replaced by D) [70Bre]. $f = 1$ kHz, 200 V m^{-1}.

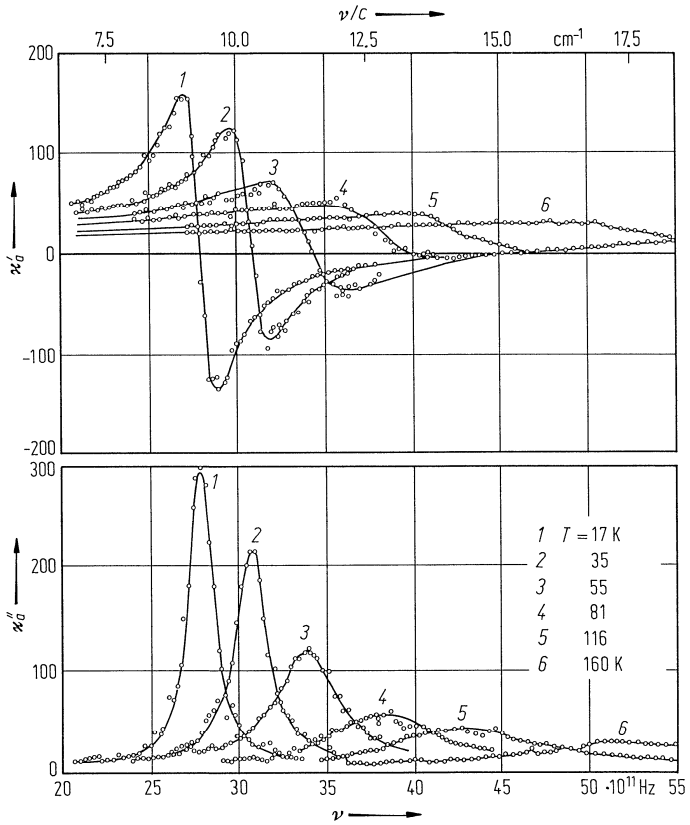

Fig. 68A-2-008. $LiTlC_4H_4O_6 \cdot H_2O$ (LTT). κ'_a, κ''_a vs. ν in a submillimeter range [86Vol]. Parameter: T. Continuous curves are calculated using a single-oscillator dispersion model.

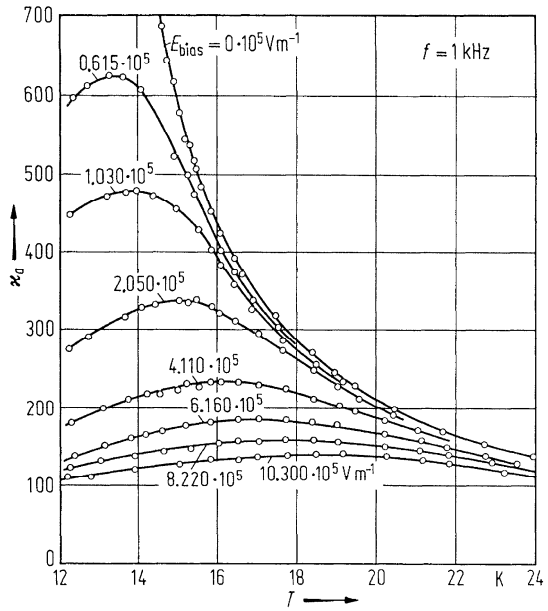

Fig. 68A-2-009. $LiTlC_4H_4O_6 \cdot H_2O$ (LTT). κ_a vs. T [70Fou]. Parameter: E_{bias}. f = 1 kHz.

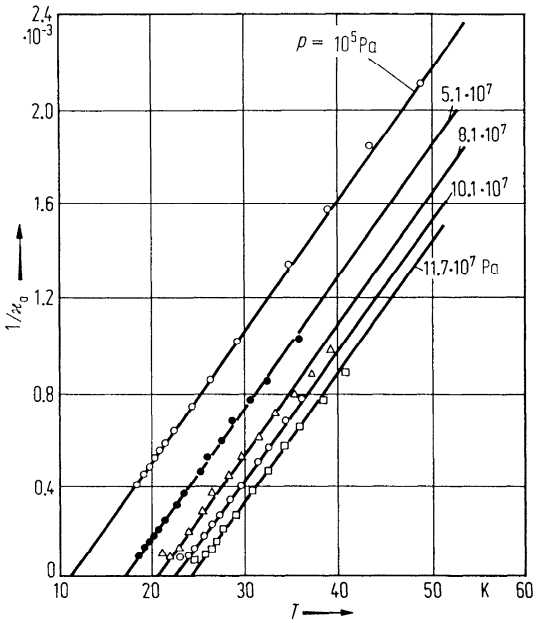

Fig. 68A-2-010. $LiTlC_4H_4O_6 \cdot H_2O$ (LTT). $1/\kappa_a$ vs. T [70Heg]. Parameter: p.

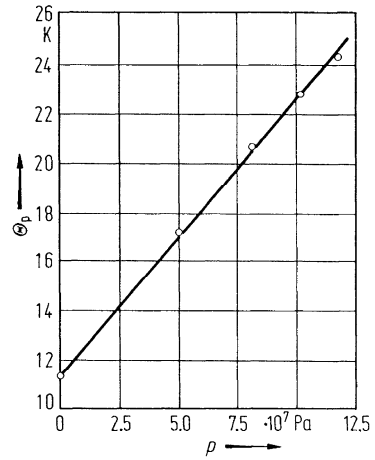

Fig. 68A-2-011. $LiTlC_4H_4O_6 \cdot H_2O$ (LTT). Θ_p vs. p [70Heg].

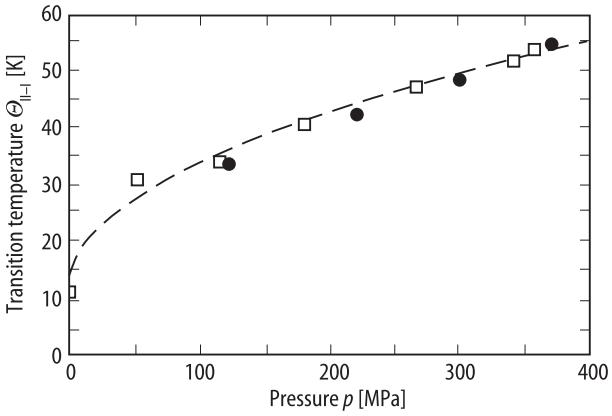

Fig. 68A-2-012. $LiTlC_4H_4O_6 \cdot H_2O$ (LTT). Θ_{II-I} vs. p [96Kam]. Open square: obtained from dielectric experiments, full circle: from Raman scattering experiment.

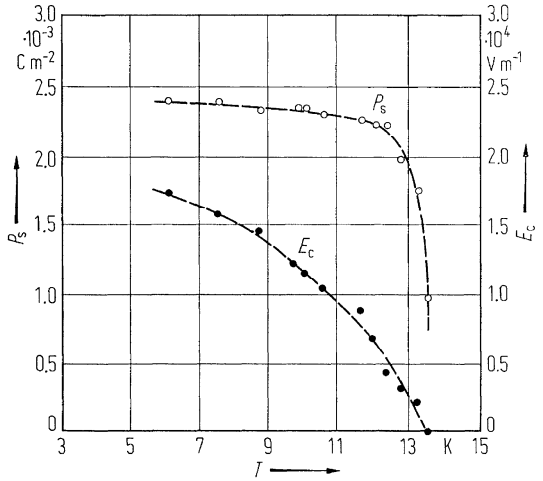

Fig. 68A-2-013. $LiTlC_4H_4O_6 \cdot H_2O$ (LTT). P_s, E_c vs. T [74Abe]. $f = 60$ Hz. Applied electric field amplitude is 120 kV m^{-1}.

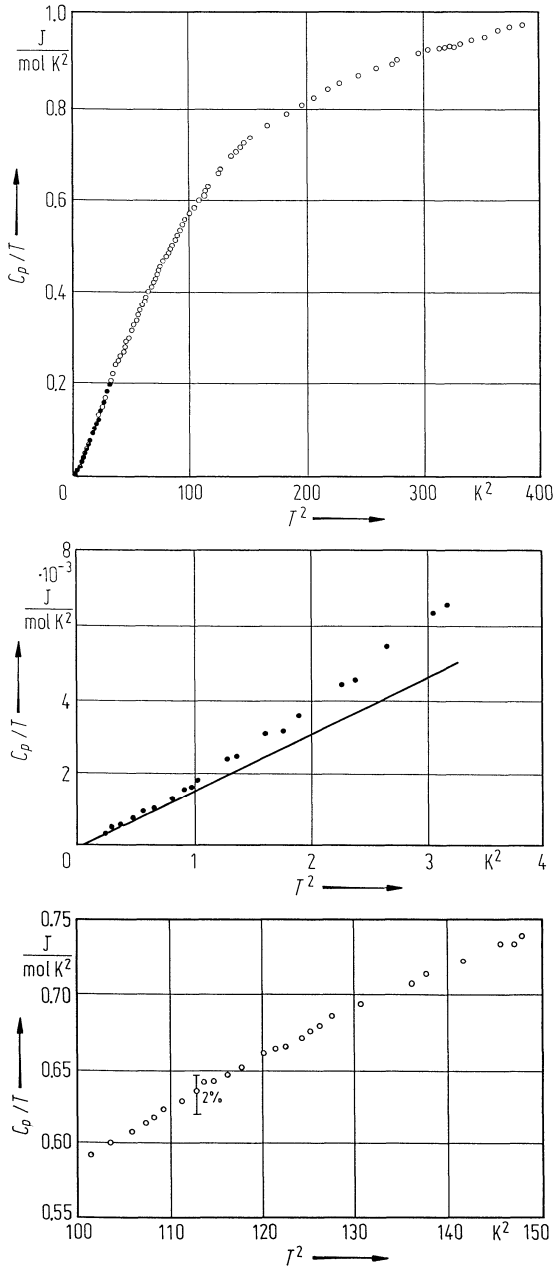

Fig. 68A-2-014. $LiTlC_4H_4O_6 \cdot H_2O$ (LTT). C_p/T vs. T^2 [80Ger]. C_p: molar heat capacity at constant pressure. Full circle: heat pulse method, open circle: ac calorimetric method. Line is a theoretical one for $\Theta_D = 110$ K.

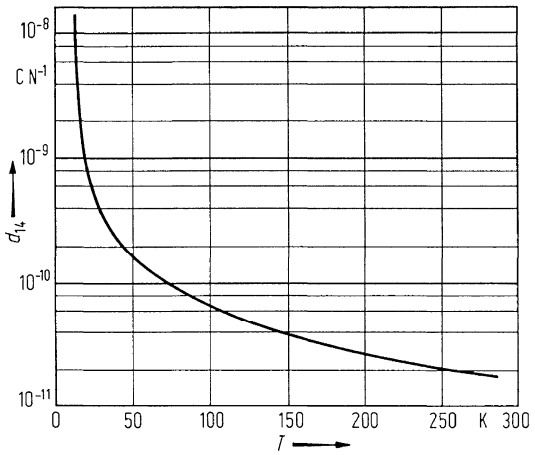

Fig. 68A-2-015. $LiTlC_4H_4O_6 \cdot H_2O$ (LTT). d_{14} vs. T [71Saw1]. d_{14}: piezoelectric strain constant.

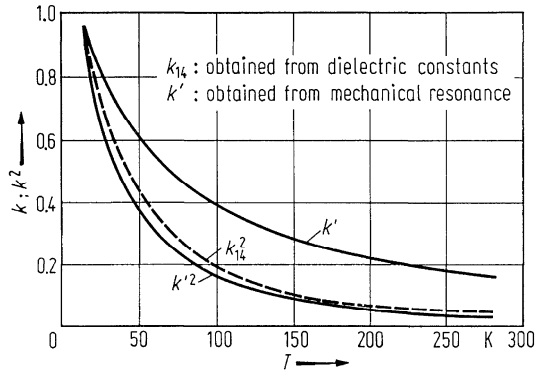

Fig. 68A-2-016. $LiTlC_4H_4O_6 \cdot H_2O$ (LTT). k, k^2 vs. T [71Saw1]. k': electromechanical coupling factor of a 45° X-cut bar for the length extensional mode of vibration. k_{14}: the coupling factor determined from $k_{14} = (1 - \kappa_a^S / \kappa_a^T)^{1/2}$.

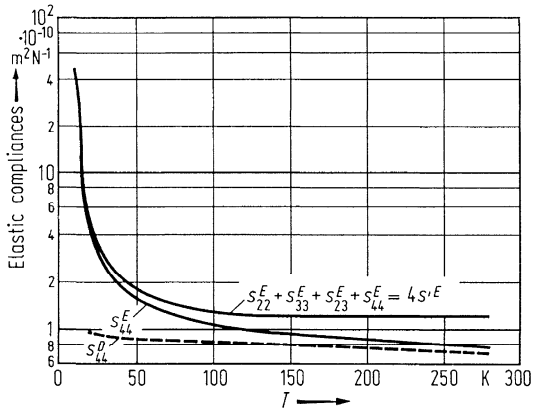

Fig. 68A-2-017. $LiTlC_4H_4O_6 \cdot H_2O$ (LTT). Elastic compliances vs. T [71Saw1]. s'^E : compliance for length extensional strain of the 45° X-cut bar at constant electric field.

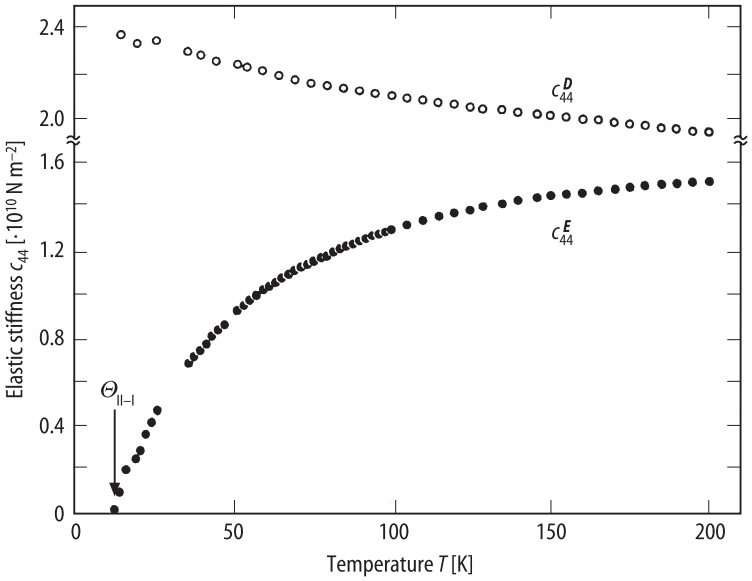

Fig. 68A-2-018. $LiTlC_4H_4O_6 \cdot H_2O$ (LTT). c_{44}^E, c_{44}^D vs. T [92Hay]. Piezoelectric resonance method.

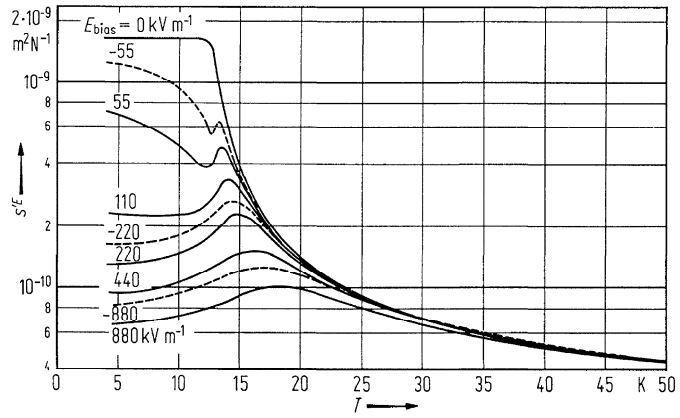

Fig. 68A-2-019. $LiTlC_4H_4O_6 \cdot H_2O$ (LTT). s'^E vs. T [71Saw2]. Parameter: E_{bias}, the dc bias field along a. $s'^E = (s_{22}^E + s_{33}^E + 2s_{23}^E + s_{44}^E)/4$.

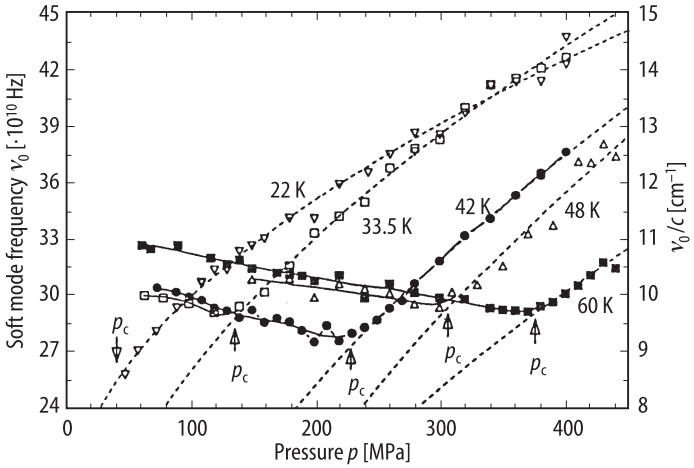

Fig. 68A-2-020. $LiTlC_4H_4O_6 \cdot H_2O$ (LTT). ν_0 vs. p [96Kam]. Parameter: T. ν_0: soft mode frequency obtained from Raman $b(cb)c$ spectra. p_c: critical pressure.

References

51Mat Matthias, B.T., Hulm, J.K.: Phys. Rev. **82** (1951) 108.
55Shi Shirane, G., Jona, F., Pepinsky, R.: Proc. IRE **43** (1955) 38.
62Bur Burns, G.: Phys. Rev. **127** (1962) 1193.
62Jon Jona, F., Shirane, G.: Ferroelectric Crystals, Oxford: Pergamon Press, 1962.
70Bre Březina, B., Janousck, V., Marecek, V., Smutny, F.: Articlc on p. 369 in Proceedings of the European Meeting on Ferroelectricity , held at Saarbrücken (1969), Müser, H.E., Petersson, J. (eds.), Stuttgart: Wissenschaftliche Verlagsgesellschaft mbH, 1970.
70Fou Fousek, J., Cross, L.E., Seely, K.: Ferroelectrics **1** (1970) 63.
70Heg Hegenbarth, E.M.: Kristallografiya **15** (1970) 322; Sov. Phys. Crystallogr. (English Transl.) **15** (1970) 268.
71McC McCarthy, G.I., Schlege, L.H., Sawaguchi, E.: J. Appl. Crystallogr. **4** (1971) 180.
71Saw1 Sawaguchi, E., Cross, L.E.: Ferroelectrics **2** (1971) 37.
71Saw2 Sawaguchi, E., Cross, L.E.: Appl. Phys. Lett. **18** (1971) 1.
72Saw Sawaguchi, E., Cross, L.E.: Article on p. 327 in Proceedings of the 1971 IEEE Symposium on Applications of Ferroelectrics, held at Yorktown Heights (1971), Cross, L.E., Kurtz, S.K. (eds.), Ferroelectrics **3** (1972) Nos. 2, 3, 4; IEEE Trans. Sonics Ultrasonics, SU **19** (1972) No. 2.
74Abe Abe, R., Kamiya, N., Matsuda, M.: Ferroelectrics **8** (1974) 557.
78Heg Hegenbarth, E., Březina, B.: Ferroelectrics **20** (1978) 181.
78Kay Kay, M.I.: Ferroelectrics **19** (1978) 159.
80Ger Gerth, B., Sahling, A., Pompe, G., Hegenbarth, E., Březina, B.: Phys. Status Solidi (a) **57** (1980) K153.
80Heg Hegenbarth, E., Spörl, G., Březina, B.: Krist. Tech. **15** (1980) K 61.
82Nov Novik, V.K., Drozhdin, S.N., Cavrilova, N.D.: Fiz. Tverd. Tela **24** (1982) 1555; Sov. Phys. Solid State (English Transl.) **24** (1982) 893.
85Toy Toyama, M., Fukui, M., Abe, R.: J. Phys. Soc. Jpn. **54** (1985) 849.
86Vol Volkov, A.A., Goncharov, Yu.G., Kozlov, G.V., Petzelt, J., Fousek, J., Březina, B.: Fiz. Tverd. Tela **28** (1986) 3185; Sov. Phys. Solid State (English Transl.) **28** (1986) 1794.
86Zhu Zhu, V., Březina, B., Günter, P.: Helv. Phys. Acta **59** (1986) 159.
88Kha Khaller, K.É, Khaav, A.A., Novik, V.K., Gavrilova, N.D.: Fiz. Tverd. Tela **30** (1988) 88; Sov. Phys. Solid State (English Transl.) **30** (1988) 47.
88Pav Pavel, M., Fousková A., Holakovský, Březina, B.: Czech. J. Phys. **B38** (1988) 314.
92Hay Hayashi, K., Deguchi, K., Nakamura, E.: J. Phys. Soc. Jpn. **61** (1992) 1357.
93Deg Deguchi, K., Nakamura, E.: J. Phys. Soc. Jpn. **62** (1993) 3392.
96Kam Kamba, S., Schaack, G., Petzelt, J., Březina, B.: J. Phys. Condens. Matter **8** (1996) 4631.

No. 68A-3 $LiKC_4H_4O_6 \cdot H_2O$, Lithium potassium tartrate monohydrate (LPT)

($M = 212.13$)

1b	phase	I	
	state	P	
	crystal system	orthorhombic	
	space group	$P2_12_12 - D_2^3$	56Zhd
	$\rho = 2.01 \cdot 10^3$ kg m^{-3}, $\rho_X = 1.981 \cdot 10^3$ kg m^{-3}.		56Zhd
2	Single crystals were grown by a slow evaporation method at room temperature from aqueous solution of equimolar mixture of lithium tartrate and potassium tartrate.		85Kuo
3a	$a = 7.855(1)$ Å, $b = 14.347(1)$ Å, $c = 6.339(1)$ Å at RT.		56Zhd
b	$Z = 4$ at RT.		56Zhd
10a	Raman scattering spectra of low frequency B_2 modes at RT: see		79Uda
	The $Y(XZ)X$ spectra at 80 K and 300 K: see		85Kuo
13b	ESR of Mn^{2+}: see		79Jai

References

56Zhd Zhdanov, G.S., Umanskii, M.M., Varfolomeeva, L.A., Ezhkova, Z.I., Zolina, Z.K.: Kristallografiya **1** (1956) 271; Sov. Phys. Crystallogr. (English Transl.) **1** (1956) 210.

79Jai Jain, A.K.: Mol. Phys. **38** (1979) 2037.

79Uda Udagawa, M., Tominaga, Y., Kohn, K., Nakamura, T., Maeda, M.: J. Phys. Soc. Jpn. **47** (1979) 869.

85Kuo Kuok, M.H., Udagawa, M., Ishibashi, Y.: Ferroelectrics Lett. **3** (1985) 129.